

1 Hyperon polarization in heavy ion collisions at STAR

2 *Xingrui Gou*^{1,*}, for the STAR Collaboration

3 ¹Institute of Frontier and Interdisciplinary Science & Key Laboratory of Particle Physics and Particle
4 Irradiation (Ministry of Education), Shandong University, Qingdao, Shandong, 266237, China

5 **Abstract.**

6 In these proceedings, we present the measurements of global polarization for
7 Λ , $\bar{\Lambda}$ with the high-statistics data collected by the STAR experiment for iso-
8 bar (Ru+Ru, Zr+Zr) collisions at $\sqrt{s_{NN}} = 200$ GeV and Au+Au collisions at
9 $\sqrt{s_{NN}} = 19.6, 27$ GeV. These measurements allow us to study possible mag-
10 netic field driven effects through the polarization difference between Λ and $\bar{\Lambda}$
11 and system size dependence of global polarization. Furthermore, we present
12 the first measurements of Λ , $\bar{\Lambda}$ hyperon local polarization in isobar collisions at
13 $\sqrt{s_{NN}} = 200$ GeV and Au+Au collisions at $\sqrt{s_{NN}} = 19.6, 27$ GeV. Comparisons
14 with previous measurements in Au+Au and Pb+Pb collisions at RHIC and LHC
15 provide important insights into the collision system size and energy dependence
16 of the vorticities. The local polarization measurements at lower beam energies
17 can probe the predicted baryonic spin hall effect in a dense baryonic environ-
18 ment in heavy-ion collisions.

19 **1 Introduction**

20 In non-central heavy-ion collisions, the produced system has large orbital angular mo-
21 mentum and may have a strong vortical structure, which leads to the global spin polarization
22 of hyperons through the spin-orbital interaction [1]. Due to the nature of the weak decay, Λ
23 hyperon's polarization can be determined through the angular distribution of decay daughter
24 proton in parent's rest frame.

25 In these proceedings, we report Λ , $\bar{\Lambda}$ global and local polarization as a function of cen-
26 trality in Au+Au collisions at $\sqrt{s_{NN}} = 19.6, 27$ GeV and Ru+Ru, Zr+Zr collisions at $\sqrt{s_{NN}}$
27 $= 200$ GeV, using the data collected by STAR experiment.

28 **2 Global polarization results**

29 In the STAR experiment, the global polarization is determined by $P_{\Lambda} = \frac{8}{\alpha\pi} \frac{1}{A^0} \frac{\langle \sin(\Psi_1 - \phi_p^*) \rangle}{\text{Res}(\Psi_1)}$
30 where α is the decay parameter, A^0 is the acceptance correction factor, ϕ_p^* is the decay proton
31 azimuthal angle in Λ s rest fame. $\text{Res}(\Psi_1)$ is the first-order event plane resolution, can be
32 determined by Zero Degree Calorimeters with Shower Maximum Detectors (ZDC SMD).
33 $\Lambda(\bar{\Lambda})$ hyperons have been reconstructed through the decay channel: $\Lambda \rightarrow \pi^- + p$ ($\bar{\Lambda} \rightarrow \pi^+ + \bar{p}$).

34 Global polarization has been observed for Λ and $\bar{\Lambda}$ hyperons in Au+Au collisions from
35 $\sqrt{s_{NN}} = 3$ to 200 GeV by the STAR experiment [2, 3]. The possible splitting between Λ

*e-mail: Gouxr@sdu.edu.cn

36 and $\bar{\Lambda}$ global polarization, expected from the magnetic field[3], is not statistically significant
 37 with the data collected in the beam energy scan I (BES-I) program. The STAR collaboration
 38 recently acquired about 10 times statistics at $\sqrt{s_{NN}} = 19.6$ and 27 GeV from BES-II compared
 39 to BES-I. Results of Λ ($\bar{\Lambda}$) global polarization as a function of collision centrality is found
 40 to increase monotonically. The polarization splitting $P_{\bar{\Lambda}} - P_{\Lambda} = -0.018 \pm 0.127(\text{stat.}) \pm$
 41 $0.024(\text{syst.})\%$ at 19.6 GeV, $P_{\bar{\Lambda}} - P_{\Lambda} = 0.109 \pm 0.118(\text{stat.}) \pm 0.022(\text{syst.})\%$ at 27 GeV,
 42 integrated over 20-50% centrality, is not statistically significant from BES-II[4].

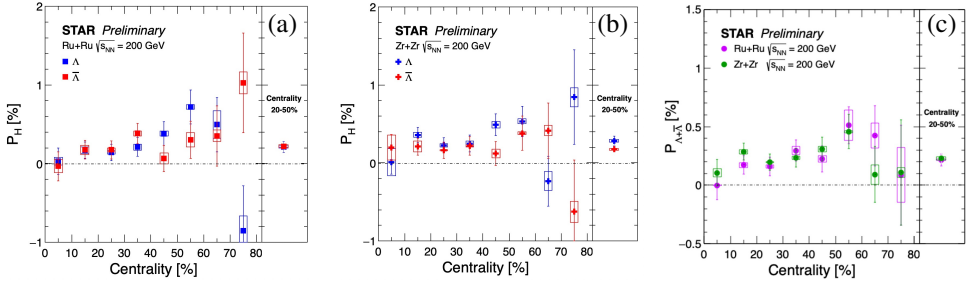


Figure 1: Global polarization of Λ and $\bar{\Lambda}$ as a function of centrality in Ru+Ru(a), Zr+Zr(b) collisions at $\sqrt{s_{NN}} = 200$ GeV. Panel (c) shows $\Lambda+\bar{\Lambda}$ global polarization results in isobar collisions. Open boxes and vertical lines represent systematic and statistical uncertainties.

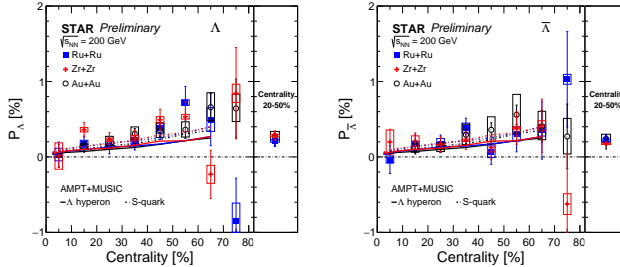


Figure 2: Λ (left) and $\bar{\Lambda}$ (right) global polarization as a function of centrality in Ru+Ru, Zr+Zr, and Au+Au collisions at $\sqrt{s_{NN}} = 200$ GeV.

43 Figure 1 (a) and (b) show Λ and $\bar{\Lambda}$ global polarization $P_{\Lambda,\bar{\Lambda}}$ as a function of centrality in
 44 Ru+Ru and Zr+Zr collisions. The polarization increase from central to peripheral collisions.
 45 In order to achieve a better precision in polarization splitting, we also combine measurements
 46 in 20-50% centrality results. No significant difference between Λ and $\bar{\Lambda}$ global polarization
 47 in Ru+Ru and Zr+Zr collisions is observed. It indicates that there is no magnetic field driven
 48 effects on the hyperon polarization within present statistical precision. Figure 1 (c) shows
 49 $\Lambda+\bar{\Lambda}$ global polarization $P_{\Lambda+\bar{\Lambda}}$ as a function of centrality in Ru+Ru and Zr+Zr collisions.
 50 The results are consistent in each centrality between Ru+Ru and Zr+Zr collisions.

51 Figure 2 shows Λ and $\bar{\Lambda}$ global polarization comparison between isobar and Au+Au
 52 collisions. The results are consistent for the whole centrality range, indicating there is no
 53 obvious collision system size dependence. The hydrodynamic model calculation from Λ
 54 polarization scenario and s -quark polarization scenario are consistent with the experiment
 55 data[5].

56 3 Local polarization results

57 STAR has measured the local polarization with respect to the second-order event plane
 58 in Au+Au collisions at $\sqrt{s_{NN}} = 200$ GeV [6]. The local polarization $\langle \cos\theta_p^* \rangle$ as a function of

59 azimuthal angle relative to the second-order event plane shows a sine modulation, as expected
60 from quadrupole structure of vorticity along the beam direction. The second and third-order
61 event planes are determined by the Time Projection Chamber detector (TPC).

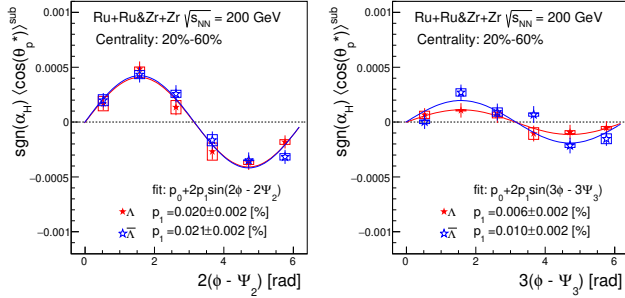


Figure 3: Local polarization $\langle \cos\theta_p^* \rangle$ of Λ and $\bar{\Lambda}$ hyperons as a function of azimuthal angle ϕ relative to the second and third-order event plane in isobar collisions at $\sqrt{s_{NN}} = 200$ GeV[7].

62 Figure 3 shows $\langle \cos\theta_p^* \rangle$ of Λ and $\bar{\Lambda}$ hyperons as a function of azimuthal angle ϕ relative
63 to the second-order event plane Ψ_2 (left) and third-order event plane Ψ_3 (right) for 20% – 60%
64 centrality, respectively. The solid lines are the fits to the results with $p_0 + 2p_1 \sin(n\phi - n\Psi_n)$.
65 The left panel in figure 3 shows a clear sine modulation in polarization signal, as expected
66 from quadrupole structure of vorticity along the beam direction. The pattern in isobar collisions
67 is similar to that in Au+Au with better statistical significance. Figure 3 (right) shows the
68 first measurements of $\langle \cos\theta_p^* \rangle$ with respect to the third-order event plane Ψ_3 . The results also
69 show a sine modulation for both Λ and $\bar{\Lambda}$, indicating triangular flow driven polarization[7].

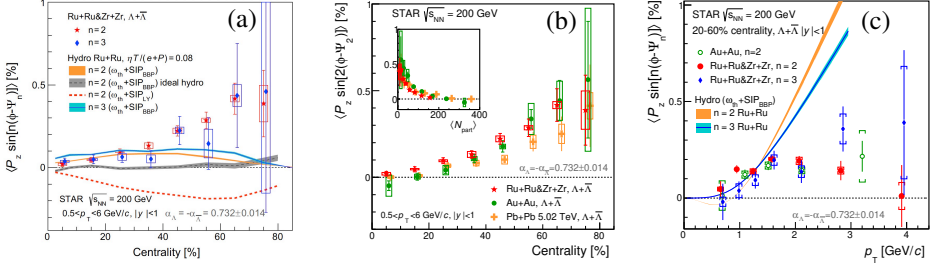


Figure 4: (a): the local polarization w.r.t 2nd(3rd) event plane of $\Lambda + \bar{\Lambda}$ as a function of the collision centrality in isobar collisions at $\sqrt{s_{NN}} = 200$ GeV. (b): the comparison of the second Fourier sine coefficient of $\Lambda + \bar{\Lambda}$ local polarization among isobar, Au+Au collisions at $\sqrt{s_{NN}} = 200$ GeV and Pb+Pb collisions at $\sqrt{s_{NN}} = 5.02$ TeV. (c): local polarization w.r.t 2nd(3rd) event plane of $\Lambda + \bar{\Lambda}$ as a function of transverse momentum. [7]

70 Figure 4 (a) presents the comparison of centrality dependence of magnitude of $\Lambda + \bar{\Lambda}$
71 local polarization with respect to second and third Fourier sine coefficients. The results from
72 second order event planes is consistent with expected increase in elliptic flow magnitude
73 towards peripheral collisions. The results from third order also increases from central to
74 peripheral collisions. However, there is no significant difference between the second-order
75 and third-order local polarization within measurement uncertainties.

76 Figure 4 (b) shows the $\Lambda + \bar{\Lambda}$ local polarization with respect to the second-order event
77 plane as a function of the collision centrality in isobar, Au+Au, and Pb+Pb collisions. A hint
78 of system size dependence has been observed when comparing isobar and Au+Au collisions
79 at $\sqrt{s_{NN}} = 200$ GeV, while the energy dependence is not obvious between $\sqrt{s_{NN}} = 200$ GeV
80 Au+Au collisions and $\sqrt{s_{NN}} = 5.02$ TeV Pb+Pb collisions.

81 The local polarization relative to both event planes are plotted as a function of hyperons
 82 transverse momentum in Figure 4 (c). Results show that p_T dependence of the polarization
 83 is indeed similar to that of elliptic (v_2) and triangular (v_3) flow.

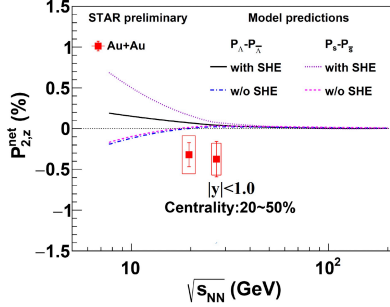


Figure 5: Net local polarization as a function of collision energy.

84 Figure 5 presents the net local polarization of Λ and $\bar{\Lambda}$, an observable designed to probe
 85 the baryonic Spin Hall effect (SHE)[5], in Au+Au collisions at $\sqrt{s_{NN}} = 19.6$ and 27 GeV
 86 using data from BES-II. The present measurement of net local polarization does not have the
 87 precision to conclude on the scenario of SHE at the measured energies. Measurements at
 88 lower energies, where SHE signal is anticipated, are currently in progress.

89 4 Summary

90 The global and local polarization of Λ and $\bar{\Lambda}$ have been measured in isobar (Ru+Ru,
 91 Zr+Zr) collisions at $\sqrt{s_{NN}} = 200$ GeV and Au+Au collisions at $\sqrt{s_{NN}} = 19.6$ and 27 GeV.
 92 The global polarization of Λ and $\bar{\Lambda}$ are consistent, indicating that the magnetic field effects on
 93 global polarization are not observed within current statistical limitation. The global polariza-
 94 tion is consistent across collisions with different system sizes, Ru+Ru, Zr+Zr, and Au+Au at
 95 same collision centrality and beam energy. Significant local polarization signals with respect
 96 to the second-order and third-order event plane are observed in isobar collisions at $\sqrt{s_{NN}} =$
 97 200 GeV. A slight hint of collision system size dependence has been observed, while energy
 98 dependence is not obvious. An observable of net local polarization, proposed to probe the
 99 baryonic Spin Hall effect, is measured in Au+Au collisions at $\sqrt{s_{NN}} = 19.6$ and 27 GeV.
 100 The present measurement of net local polarization does not have the precision to conclude on
 101 the scenario of SHE at the measured energies. Global and local polarization studies at other
 102 BES-II energies are underway.

103 Acknowledgements

104 The author is supported by the National Key Research and Development Program of
 105 China (Grant No. 2022FYA1604903)

106 References

- 107 [1] Z. T. Liang and X. N. Wang, Phys. Rev. Lett. 94,102301 (2005); 96, 039901(E) (2006).
 108 [2] L. Adamczyk et al., (STAR Collaboration), Nature 548, 62 (2017).
 109 [3] J. Adam et al., (STAR Collaboration), Phys. Rev. C 98, 014910 (2018).
 110 [4] J. Adam et al., (STAR Collaboration), Phys.Rev.C 108 1, 014910 (2023).
 111 [5] B. Fu et al, arXiv: 2201.12970 (2022).
 112 [6] J. Adam et al., (STAR Collaboration), Phys. Rev. Lett. 123, 132301(2019)
 113 [7] J. Adam et al., (STAR Collaboration), Phys. Rev. Lett. 131, 202301(2023)